Control Investigations of Rotor Supported by AMBs During Severe Foundation Excitations

Clément Jarroux [a], Jarir Mahfoud [a], Benjamin Defoy [b] and Thomas Alban [b]

[a] Univ Lyon, INSA Lyon, CNRS UMR5259, LaMCoS, F-69621, France, jarir.mahfoud@insa-lyon.fr
[b] GE Oil & Gas, 480 Avenue Gustave Eiffel, 71200 Le Creusot, France

***Abstract*—The study is devoted to numerical and experimental investigations of the dynamic behavior of base excited rotating machines supported by Active Magnetic Bearings (AMBs). In case of strong base motions, the rotor can contact its touchdown bearings (TDBs) which are emergency bearings. The objective is to analyze the effect of the combination of mass unbalance forces, base motion excitations and contact nonlinearities on a rotor-AMB system response. In particular, the capacity of an augmented PID controller to maintain the system stable. FE method was developed to model the on-board rotor-AMB system. An academic scale test rig was used for the experimental investigations. Predicted and measured responses due to impulse excitations applied on the foundations were compared. The capacity of the controller to maintain the system stability is discussed.**

I. INTRODUCTION

Due to the progress made in electronics, AMBs are now widely used in different industrial applications and have been successfully implemented in the field of turbomachinery [1-3]. They are contact-less, no sealing constraints, frictionless suspension, and that they constitute an active system. On the other hand, AMBs produce only electromagnetic attraction and have nonlinear characteristics; therefore, AMBs are inherently unstable and require feedback control and special attention to the global environment to ensure stable operation [4]. Several studies have been devoted to the elaboration of new controllers that enable better design and performance in operating situations, with acceptable levels of stability and robustness [5-8]. The augmented PID controller is still widely used in industrial applications, since it permits designers to master the control process. However, the control of flexible rotors remains difficult due to unavoidable spillover effects. This problem is currently overcame by using phase lag and phase lead filters [9]. In this case, tuning these controllers is a delicate operation and is time consuming.

Depending on the targeted applications, rotating machines may have to face more or less severe environmental conditions. Turbomachinery used for the electrical production in nuclear plant may deal with earthquake such as the recent events of Fukushima where the station was deeply damaged. Also regarding the offshore platform such as floating production storage and offloading where the floating vessels could be subjected to large structural vibrations during storms, or due to large waves. In these cases, the integrity of turbomachinery may be affected and the dynamic behavior of on-board rotating machines should be carefully analyzed and optimized in order improve the reliability, and to maintain a maximal operability of the machines.

Many studies focused on the dynamic behavior of rotors subjected to their external environment [10-12]. Generally, industrial supports are rigid and the transmissibility to the rotor is then high; the dynamic contributions of the foundation may be neglected. However, some works consider flexible supports [13]. Considering harmonic rotational base motions, at certain frequencies of the support combined with the natural frequencies of the rotor, instability zones emerge and depend on the amplitude of the rotation angle [14-16].

Several works were dedicated to the implementation of different control strategies to limit the base motions and avoid TDBs interactions. Must often, a feedforward compensator is added to the conventional controllers [17–21] or the control strategy is adapted to reduce base motions such as in references [22-24]. The effect of base disturbances when the control strategy was not specifically tuned for that purpose was also assesses [25]. In most of these studies, the rotor response due to base motions remained small, either because a specific control strategy was applied to reject external disturbances or because the acceleration levels tested remained quite small. Even if the nonlinearity of magnetic forces was exhibited in some cases, few studies have considered rotor-TDB interaction due to base motions while AMBs still operate. To the best of author's knowledge, it was numerically investigated by Hawkins [26].

This work is a part of a research project aiming at contributing to the improvement of knowledge concerning the dynamic behavior of turbomachinery supported by AMBs when subjected to external events. In particular, the dynamic behavior of a rotor-AMB system subjected to strong base motion leading the rotor to contact TDB while AMB still operate. The objective is to analyze the effect of the combination of mass unbalance forces, base motion excitations and contact nonlinearities on a rotor-AMB system response and the capacity of an augmented PID controller to maintain the system stable. A Finite Element model was developed in order to simulate and optimized the dynamic behavior. The mode is then validate through experimental investigations using an experimental academic test rig. The validation tests were carried out by applying vertical impulse excitations to the system base. The capacity of the controller to maintain the system in stable operating conditions is then discussed.

II. MODELLING

The different models were necessary to perform transient simulations considering a rotor-AMB system subjected to external disturbances and potential TDB contacts. The modelling approach is modular and each model can be either employed or not in the simulations.

The rotor is composed of shaft, bearings, discs, and unbalance distribution, and the support. It is assumed that: the shaft is flexible and modelled by beam elements for lateral analysis; the discs are rigid and symmetric; the unbalance distribution is modelled by discrete masses and the support is rigid but mobile.

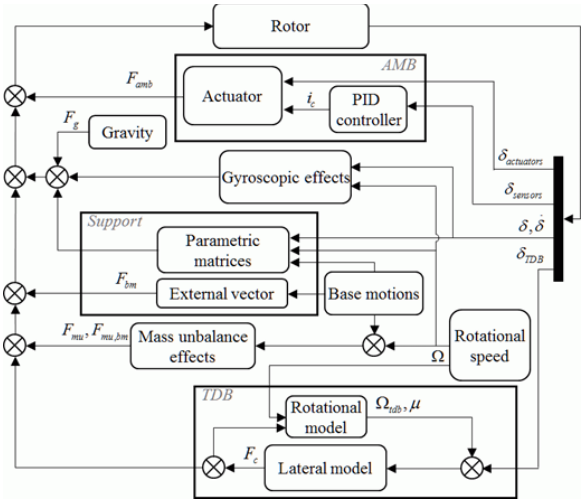

Figure 1. Modelling approch

The modelling approach used is presented in figure 1. The nonlinear contributions such us the additional forces due to the base motion (support block) or the efforts due to the contact of the rotor with the TDB are considered as restoring forces. It was the same concerning the forces delivered by the AMB. The gravity as well as the gyroscopic effects were also considered in the second member of the equation of motion. This modelling approach enable to have a linear part concerning the rotor, consequently, the modal reduction can be applied easily

To derive the different energies of each components of the rotor, the instantaneous angular velocity vector and the position vector are expressed with respect to the Galilean frame in the rigid support frame. The energetic contribution and the virtual work of each components are calculated. The flexible shaft contributes with the kinetic and strain energies, it is modeled with 41 Timoshenko beam elements with two nodes and 4 d.o.f. per node; the discs with the kinetic energy; the discrete mass unbalances with the kinetic energy, and the bearing restoring forces with the virtual work. The base motions modify only the kinetic energies. Once the energies are set-up, they are derived by using the Lagrange's equations leading to the equations of motion as [27]:

$$M\ddot{\delta}+\left(\Omega C^{g}+\omega^{y}C_{bm}^{\omega^{y}}\right)\dot{\delta}+\left(K^{e}+\dot{\omega}^{y}K_{bm}^{\dot{\omega}^{y}}+\Omega\,\omega^{y}K_{bm}^{\Omega\omega^{y}}\right.$$
$$\left.+\omega^{x2}K_{bm}^{\omega^{x2}}+\omega^{y2}K_{bm}^{\omega^{y2}}+\omega^{z2}K_{bm}^{\omega^{z2}}+\omega^{x}\omega^{z}K_{bm}^{\omega^{x}\omega^{z}}\right)\delta=$$
$$F_{mu}+F_{bm}+F_{g}+F_{amb}+F_{c} \qquad (1)$$

with M, K^e and C^g are respectively the mass, the structural stiffness and the gyroscopic matrices. Ω is the rotational speed, $\delta,\dot{\delta},\ddot{\delta}$ are displacement, velocity and acceleration. $\omega^{x;y;z}$ is the rotational speed of the support along the direction x, y or z. C_{bm}^{ω} , K_{bm}^{ω} are the additional (gyroscopic or stiffness) matrices due to the support rotations. F_{mu} is the mass unbalance force vector taking into account the normal centrifugal and tangential centripetal forces. The subscript *bm* stands for the base motions effects. The external force vector F_{bm} contains all the contribution of the translations of the support combined with its rotations, F_g the effect of gravity, F_c represents the TDBs contact force vectors. F_{amb} the forces delivered by the AMBs, which is the output of an augmented PID and takes into account the characteristics of the utilized AMBs.

Fc is obtained by modelling the TDBs with normal and tangential forces (f_n, f_t):

$$f_n=\begin{cases}k_{brg}\left(\delta_{rs}-\delta_{rd}\right)+c_{brg}\dot{\delta}+k_{eq}\delta_{rd} & ;\ \delta_{rs}\geq\delta_{rd}\\ k_{eq}\delta_{rs}+c_{eq}\dot{\delta}_{rs} & ;\ \delta_{rd}>\delta_{rs}\geq 0\\ 0 & ;\ \delta_{rs}>0\end{cases} \qquad (2)$$

$$f_t=\begin{cases}\mu\ f_n & \delta_{rs}\geq 0\\ 0 & \delta_{rs}<0\end{cases}$$

where δ_{rs} is the rotor-TDB relative clearance and δ_{rd} is the ribbon crushing capacity, k_{brg}, c_{brg} the dynamic parameters of the ball bearing.

When the rotor interacts with the TDB, it first contacts the coupled ball bearing ribbon damper system, considered in series mode. The related contact force is composed of the equivalent stiffness k_{eq} and damping c_{eq}. The tangential contact force model f_t considers the sliding friction generated at the rotor-TDB interface due to different rotational speeds and considers the tangential damping provided by the ribbon damper counteracting the rotor whirl. μ is the sliding friction coefficient that takes into account the dry and the dynamic friction coefficient, associated with a reduced and a large sliding velocity [27].

F_{amb} is generated along each action lines and depends on the air gap g_0 and the applied current in the coils. The latter being the sum/subtraction of a control current i_c and a constant bias current I_0, as electromagnets are used in differential driving mode.

$$f_{amb}=4\,\mu_0\cos\alpha\,S\,N^2\left[\frac{(I_0-i_c)^2}{\left(\frac{L}{\mu_R}+2g_0-2x\cos\alpha\right)^2}-\frac{(I_0+i_c)^2}{\left(\frac{L}{\mu_R}+2g_0+2x\cos\alpha\right)^2}\right] \qquad (3)$$

Where μ_0 the permeability of vacuum space, *S* the pole area, *N* the number of turn in one coil, *x* the rotor position, μ_r the relative permeability of the iron core, *L* the average length of magnetic flux lines and α the angle between the action line and the line joining the pole and the rotor centres respectively.

An augmented PID was modelled for the controller with the displacements as Input and the control current as output (Fig.2).

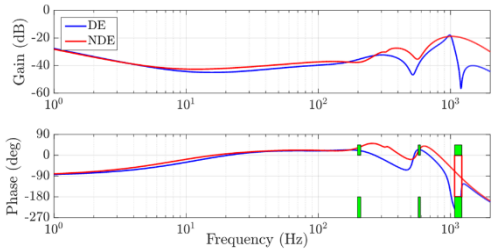

Figure 2. Controller transfer function

The controller characteristics are determined as a function of the dynamic behaviour and the number of modes included in the operating conditions [28]. Also, the stiffness is chosen low and the damping is concentrated around the system natural frequencies. The high frequency stability and robustness depend on the mode shapes and frequencies. The parameters that provide a suitable behaviour are specific to each bearing that is managed by tuning lead-lag filters for each bearing.

The electronic part of AMB is represented with a first order low pass filter with a cut off frequency of 2kHz. This transfer function takes into account the displacement probe bandwidth, the time delay introduced by digital signal processor and the amplifier response.

III. EXPERIMENTAL SETUP

The experiments were performed using an academic test rig, which is a commercial product manufactured by SKF® delivered with a dedicated PID controller (Fig.3). The test rig is equipped with two identical AMB called NDE (Non Drive End) and DE (Drive End) bearings. Each bearing has a maximum static capability of 280 N with air gaps of 0.432 mm. The action lines are positioned in the configuration load between axes. They are powered in differential driving mode with a bias current of 1A. Currents are provided in the range of 0-3A using PWM amplifiers. Two displacement sensors (variable reluctance probes) are integrated in the housing of each bearing and are non-colocalized with actuators. Each AMB has one back-up bearing with a clearance radius of 0.1mm.

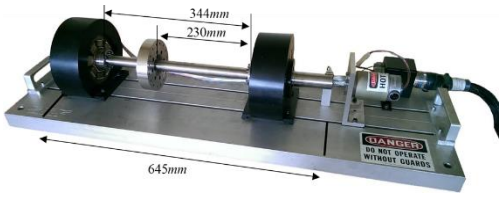

Figure 3. Academic test rig

The shaft is composed of three parts bolted together. A central part (diameter: 25mm; length 344mm) with a decentered disc 120mm in diameter and 25mm long placed at two-thirds of the central part length from the DE side, together with two shaft ends (50mm of main diameter). The stack of laminated steel sheets is shrunk on each of these two shafts. The total rotor length is 645mm. The rotor mass is 6.5kg. The rotor is driven by a 500W electric motor with a maximum speed of 12,600rpm. The operating speed range used in this work is 0 to 9,500rpm, which includes two first rigid modes. The speed of the rotor is monitored by using a speed sensor placed close to the motor.

To perform base motion tests, the academic test rig is mounted on a 6-axis hydraulic shaker (Fig. 4), which is a fully integrated system. It has 6 real-time pilots able to apply various combinations of solicitations along and around the 3 axes (translations and rotations) to a maximum mass of 450 kg in a range [0-250] Hz. A maximum acceleration of 10 G, ± 50 mm in translation and ± 4 degrees in rotation can be generated.

The data acquisition system of the shaker was used. Base accelerations were recorded in the three directions (Xcube, Ycube, Zcube) using four tri-axial accelerometers fixed on the shaker. The displacement and current sensors for each action line (V13, W13, V24, W24), and the rotational speed were also recorded. The sampling frequency was set to 24,756 Hz.

Figure 4. Experimental test rig on the hydraulic shaker

IV. RESULTS

First, the measured and the predicted displacements were compared. The aim was, to check if the proposed modelling approach could represent the observed phenomena, and to evaluate the capability of the controller used to keep stable operating conditions in the presence of base motion and contact between the rotor and the TDBs.

Then, and as the AMB capacity was oversized with respect to the studied system, the controller is assed, only numerically, when using AMB with lower capacity adapted to the rotor studied.

A. Model Validation

Measured and predicted rotor vertical displacements were compared. The tests were carried out in vertical translation by using impulse excitations. The shock lasted 0.02 s (50 Hz) and increased from 0.5 to the set value of 3.1 G. Once the acceleration set level reached, ten shocks were repeated each second (Fig. 5). The rotor speed was set to 9,500 rpm.

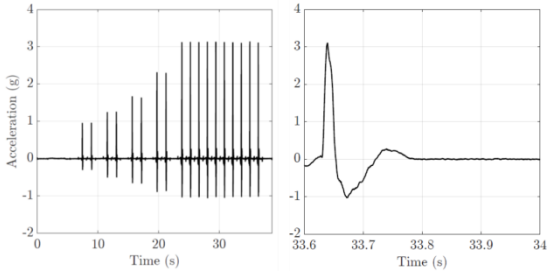

Figure 5. Measured repeated shocks and zoom, 3.1 G at 50 Hz

The accelerations recorded on the shaker were implemented in the numerical model. The predicted and measured vertical rotor displacements are presented in figure 6 for the accelerations levels applied. Predictions are close to

measurements. At 1 G acceleration level, the rotor reaches the TDBs and the maximal displacement is flattened (Fig. 6).

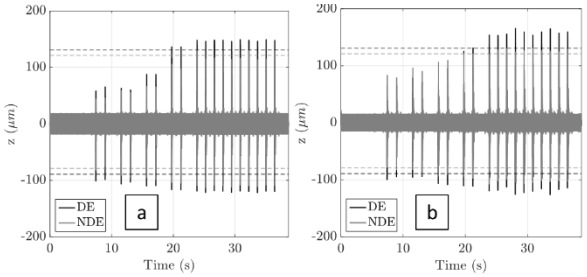

Figure 6. Predicted (a) vs measured (b) vertical rotor displacements (solid lines) and TDB clearances (dotted lines) - 9 500 rpm and 3.1 G at 50 Hz

When reaching 1.4 G, the ribbon is fully crushed during the contact at the DE side. From 1.9 G, a change of slope is observed at the DE side (Fig.7). The model seems to be able to predict the dynamic behavior of the rotor under severe excitation.

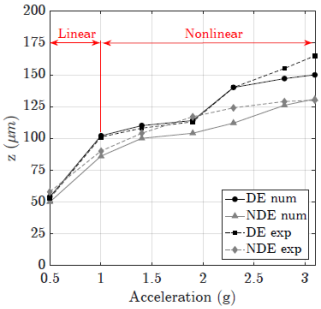

Figure 7. Measured and predicted maximal vertical rotor displacements

The measured and predicted displacements were compared when reaching the acceleration set level.

Figure 8 is a zoom of the displacement with the profile of the acceleration excitation applied. First, good agreement could be noticed between measurements and numerical simulations. The model describes closely the dynamic behavior in both amplitude level and the transient domain (attenuation and rebounds number).

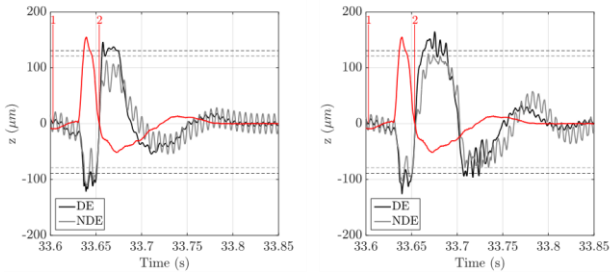

Figure 8. Predicted vs measured displacements, and acceleration profile, 9500 rpm and 3.1 G at 50 Hz

Second, the controller (augmented PID) seems to be efficient and was able to maintain the system stable during and after the application of the excitation.

B. *Controller Validation*

It is worth mentioning that the dynamic capacity of the AMB (280 N) is largely oversized with respect to the studied system. In order to check the capacity of the AMBs, when they were designed as a function of the rotor weight and expected excitations, numerical simulations were carried out (downsized). The needed dynamic capacity was calculated, and was found almost half the used one. Therefore, to reduce the dynamic capacity, the air gap was increased from of 0.432 mm to 0.611 mm and the new capacity was set to 140 N.

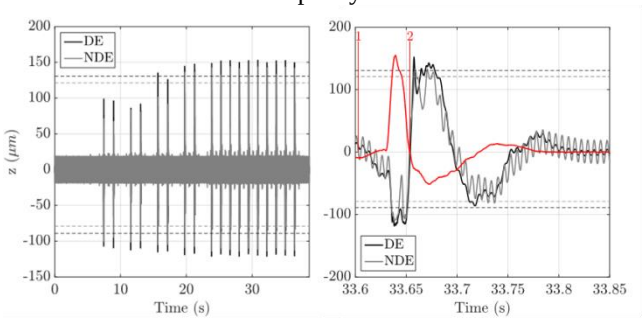

Figure 9. Predicted displacements, and acceleration profile, 9500 rpm and 3.1 G at 50 Hz

The calculations were then performed in the same conditions and for the same configuration of excitation. Here also the AMB was able to maintain the system stable as it could be seen in figure 9. Only the transient domain was slightly longer. The maximum amplitude level still unchanged since the displacements were limited by the TDBs.

V. CONCLUSIONS

The aim was to investigate experimentally and numerically the nonlinear dynamics of a rotor supported by Active Magnetic Bearings and subjected to severe motions from its foundations. The test configurations were carried out in vertical translation by using impulse excitations. The PID controller was tuned for conventional operating conditions, and no specific work on the control loop was done. The aim was to check if the control could be able to withstand the nonlinearities due to the contact.

The model developed was able to reproduce the overall dynamics and the main observed phenomena considering an academic on-board rotor-AMB system. The model describes closely the dynamic behavior in both amplitude level and the transient domain regarding the attenuation and the rebounds number.

AMBs were kept operational during the application of the excitation and the contact between the rotor and the TDBs. The PID controller was able to keep the system stable during and after the application of the excitations.

As AMBs were oversized for the studied system, numerical simulations, in the same configurations, were carried out again by using AMBs with lower dynamic capacity. The new capacity corresponds to the required one for test rig studied. This task was achieved by increasing the air gap distance. The actuators were still able to maintain the stability of the system, and only the transient domain was slightly longer.

REFERENCES

[1] G. Schweitzer and E. H. Maslen, "Magnetic Bearings, Theory, Design, and Application to Rotating Machinery", *Springer-Verlag*, 535p, 2009.

[2] M. K. Swann, A. P. Sarichev and E. Tsunoda, "A diffusion model for active magnetic bearing systems in large turbomachinery" *Proceeding 11th ISMB, Japan*, pp. 380-384, 2008.

[3] A. Masala, G. Vannini, M. Lacour, F.M. Tassel and M. Camatti, "Lateral Rotordynamic Analysis and Testing of a Vertical High Speed 12.5MW Motorcompressor Levitated by Active Magnetic Bearings", *Proceeding of the 12th ISMB, China* , 2010.

[4] E. Maslen, P. Hermann, M. Scott and R. Humphris, "Practical limits to the performance of magnetic bearings: peak force, slew rate and displacement sensitivity", *ASME Journal of Tribology*, Vol. 111, No. 2, pp. 331-336, 1989.

[5] B. Defoy, T. Alban and J. Mahfoud, "Assessment of the Effectiveness of a Polar Fuzzy Ap-proach for the Control of Centrifugal Compressors", *ASME Journal of Dynamic Systems, Measurement, and Control*, vol. 136, 041004-1 – 041004-8 (2014).

[6] K. Chen, P. Tung, M. Tsai and Y. Fan, "A self-tuning fuzzy PID-type controller design for unbalance compensation in an active magnetic bearing", *Expert Syst. Appl*., pp. 8560-8570, 2009.

[7] N. M. Sahinkaya, A.-H. G. Abulrub, C. R. Burrows and P. S. Keogh, "A Multiobjective Adaptive Controller for Magnetic Bearing Systems", *J. Eng. Gas Turbines Power*, 132, 122503, 2010.

[8] S. Lei and A. B. Palazzolo. Control of flexible rotor systems with active magnetic bearings", *Journal of Sound and Vibration*, Vol. 314, Issues 1-2, pp.19-38, 2008.

[9] M. Spirig, J. Schmied, P. Jenckel and U. Kanne, "Three practical examples of magnetic bearing control design using a modern tool", *ASME J. of Eng. for Gas Turbines and Power*, Vol. 124, Issue 4, pp. 1025-1031, 2002.

[10] A. S. Das, J. K. Dutt, and K. Ray, "Active vibration control of unbalanced flexible rotor-shaft systems parametrically excited due to base motion", *Applied Mathematical Modelling*, 34(9), 2353–2369, 2010.

[11] M. O. T. Cole, P. S. Keogh and C. R. Burrows, "Vibration control of a flexible rotor/magnetic bearing system subject to direct forcing and base motion disturbances", *Proceedings of the Institution of Mechanical Engineers, Part C: Journal of Mechanical Engineering Science*, 212(7), 535–546, 1998.

[12] L. A. Hawkins, B. Murphy, J. Zierer, and R. Hayes, "Shock and vibration testing of an AMB supported energy storage flywheel", *JSME International Journal Series C Mechanical Sys-tems, Machine Elements and Manufacturing*, 46(2), 429–435, 2003.

[13] K.L.Cavalca, P.F.Cavalcante and E. P. Okabe, "An investigation on the influence of the supporting structure on the dynamics of the rotor system", *Mechanical Systems and Signal Processing*, 19(1), pp. 157–174, 2005.

[14] M. Dakel, S. Baguet and R. Dufour, "Steady-state dynamic behavior of an on-board rotor under combined base motions", *Journal of Vibration and Control*, 20(15), pp. 2254–2287, 2014.

[15] N. Driot, C.H. Lamarque and A. Berlioz, "Theoretical and experimental analysis of a base-excited rotor", *Journal of Computational and Nonlinear Dynamics*, 1, pp. 257–263, 2006.

[16] Q. Han and F. Chu, "Parametric instability of flexible rotor-bearing system under time-periodic base angular motions", *Applied Mathematical Modelling*, 39(15), pp. 4511–4522, 2015.

[17] Y. Suzuki, "Acceleration feedforward control for active magnetic bearing systems excited by ground motion", *IEE Proceedings - Control Theory and Applications*, 145(2), pp. 113–118, 1998..

[18] O. Matsushita, T. Imashima, Y. Hisanaga and H. Okubo, "Aseismic vibration control of flexible rotors using active magnetic bearing", *Journal of Vibration and Acoustics*, 124(1), pp. 49–57. 10.1115/1.1423633, 2001.

[19] H.S. Kim, H.Y. Kim, C.W. Lee, C and T.H. Kang, "Stabilization of active magnetic bearing system subject to base motion"., Proceeding of the *ASME International Design Engineering Technical Conferences and Computers and Information in Engineering Conference*, no. 37033, pp. 2007–2013. 10.1115/DETC2003/VIB-48546, 2003.

[20] S. Marx and C. Nataraj, "Suppression of base excitation of rotors on magnetic bearings", *International Journal of Rotating Machinery*, p. 10 , 2007.

[21] M.S. Kang and W.H. Yoon, W, "Acceleration feedforward control in active magnetic bearing system subject to base motion by filtered-x lms algorithm", *IEEE Transactions on Control Systems Technology*, 14(1), pp. 134–140, 2006.

[22] M.O.T. Cole,P.S. Keogh and C.R. Burrows, "Vibration control of a flexible rotor/magnetic bearing system subject to direct forcing and base motion disturbances", *Proceedings of the Institution of Mechanical Engineers, Part C: Journal of Mechanical Engineering Science*, 212(7), pp. 535–546, 1998.

[23] M.S. Kang, J. Lyou and J.K. Lee, "Sliding mode control for an active magnetic bearing system subject to base motion", *Mechatronics*, 20(1), pp. 171–178, 2010.

[24] P.S. Keogh, M. Necip, S. Clifford, C.R. Burrows and S. Prabhakar, "Wavelet based adaptation of h-infinity control in flexible rotor/magnetic bearing systems", *Proceeding 7th IFToMM International Conference on Rotor Dynamics*, 2006.

[25] L.A. Hawkins, R.K. Khatri and K.B. Nambiar, "Test results and analytical predictions for mil-std-167 vibration testing of a direct drive compressor supported on magnetic bearings", *Journal of Engineering for Gas Turbines and Power*, 137(5), pp. 052507–052507–8. 10.1115/1.4028684, 2015.

[26] L.A. Hawkins, "Shock analysis for a homopolar, permanent magnet bias magnetic bearing system", *proceeding of ASME Turbo Expo 1997: Power for Land, Sea and Air*, no. 78712, p. V004T14A040. 10.1115/97-GT-230 , 1997.

[27] C. Jarroux, "Nonlinear transient dynamics of on-board rotors supported by active magnetic bearings", *PhD dissertation, INSA Lyon*, Lyon 2017.

[28] B. Defoy, "Investigation on the Control of Supercritical Centrifugal Compressors supported by Active Magnetic Bearings: Toward a new Control Strategy?", *PhD dissertation, INSA Lyon*, Lyon 2012.